Spectroscopy and Photochemistry; General Theory

Ultrafast Structure and Dynamics in the Thermally Activated Delayed Fluorescence of a Carbene-Metal-Amide

Christopher R. Hall, Alexander S. Romanov, Manfred Bochmann, and Stephen R. Meech

J. Phys. Chem. Lett., **Just Accepted Manuscript** • DOI: 10.1021/acs.jpclett.8b02797 • Publication Date (Web): 19 Sep 2018

Ultrafast Structure and Dynamics in the Thermally Activated Delayed Fluorescence of a Carbene-Metal-Amide

Christopher R. Hall,† Alexander S. Romanov, Manfred Bochmann* and Stephen R. Meech*

School of Chemistry, University of East Anglia, Norwich NR4 7TJ, UK

Abstract: Thermally activated delayed fluorescence has enormous potential for the development of efficient light emitting diodes. A recently discovered class of molecules (the carbene – metal – amides, CMAs) are exceptionally promising as they combine the small singlet - triplet energy gap required for thermal activation with a large transition moment for emission. Calculations suggest excited state structural dynamics modulate the critical coupling between singlet and triplet, but disagree on the nature of those dynamics. Here we report ultrafast time-resolved transient absorption and Raman studies of CMA photodynamics. The measurements reveal complex structural evolution following intersystem crossing on the tens to hundreds of picoseconds timescale, and a change in the low-frequency vibrational spectrum between singlet and triplet states. The latter is assigned to changes in Raman active modes localized on the metal centre.

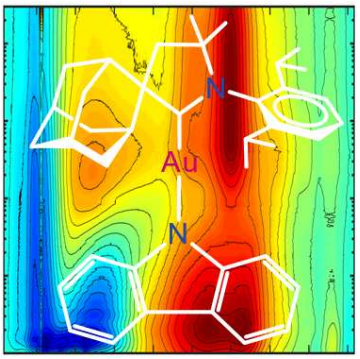

* Authors for Correspondence (m.bochmann@uea.ac.uk; s.meech@uea.ac.uk)

†Present Address: ARC Centre of Excellence in Exciton Science, School of Chemistry, The University of Melbourne, Parkville, Victoria 3010, Australia

Molecules that exhibit thermally activated delayed fluorescence (TADF) by means of reverse intersystem crossing (RISC) are critical components in organic light emitting diodes.[1-2] In the conversion of electricity to light, excitations populating triplet states are lost to emission, due to the low transition moment and competing radiationless processes. In TADF triplet excitations contribute through RISC to an emissive singlet, enhancing conversion efficiency fourfold. This requires a combination of properties including low singlet-triplet energy barrier (ΔE_{ST}), large cross section for RISC and high transition moment for fluorescence.[1, 3]

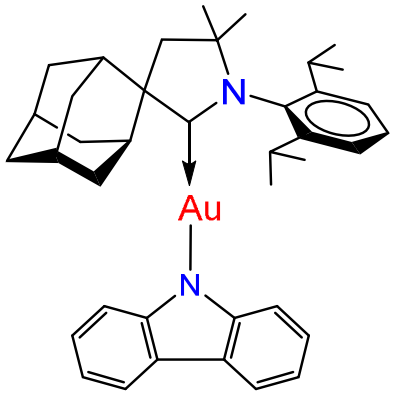

Scheme 1 *Structure of CMA1*

The Carbene – Metal – Amides (CMAs) exhibit these requirements to an unusually high degree.[4-5] CMAs consist of copper, silver or gold ions coordinated to a carbazolate anion and carbene ligand, which acts as strong σ-donor and, by virtue of its empty carbon p-orbital, an acceptor (Scheme 1). Excitation involves ligand-to-ligand charge transfer (LLCT), in which the molecular dipole moment is reduced in magnitude and reversed in direction.[4] CMA based OLED devices have been fabricated with near-100% internal quantum efficiency and short (sub-microsecond) excited state lifetimes.[4] These findings stimulated intense activity in theory and experiment, aimed at understanding this unique photophysical behaviour, and optimising efficiency of TADF in CMAs. The excited state structure of CMAs, how it evolves with time and how that evolution modifies TADF have emerged as critical aspects. Calculations point to a role for excited state bending and twisting of substituents about the central metal atom.[6-8] However, they reach different conclusions on how structural

evolution modifies TADF, indicating the need for measurements of structural dynamics. Here we provide the first such insight through ultrafast Transient Absorption (TA)[9-10] and Femtosecond Stimulated Raman Spectroscopy (FSRS),[10-12] applied to one of the most efficient CMAs (CMA1, Scheme 1). CMA1 was synthesised[5, 13] and characterised in device applications and through TA, Raman and photoluminescence.[4-5] Here we show that the femtosecond to nanosecond TA kinetics in CMA1 are more complex than for simple TADF, revealing structural evolution after ISC, and that singlet and triplet excited states show significant differences in low-frequency vibrational spectra.

Figure 1A displays steady-state and time-resolved measurements of CMA1 in chlorobenzene. The emission is a single broad band with an approximate mirror image relationship to the lowest energy absorption, with a Stokes loss of 126 nm (ca 6300 cm^{-1}). Such a large Stokes loss in a slightly polar solvent suggests a structure change between absorbing and emitting states. Figure 1B shows TA difference spectra following excitation at 405 nm (80 fs, 400 nJ/pulse, see supplementary information, SI); Fig 1C shows kinetics at selected wavelengths. At around 400 nm a ground state bleach (negative ΔA) is observed at $t = 0$, which recovers about 50% in 500 ps and then remains constant, reflecting population trapped in the long-lived (350 ns[4]) triplet state. Around 480 nm there is a second apparent bleach, assigned to stimulated emission on the basis of its match to the emission. This evolves into a TA within 10 ps, subsequently decaying to a constant level after 500 ps. Around 650 nm there is a prompt (i.e. formed within the <100 fs time resolution) TA, characteristic of excited state absorption, which initially decays in <10 ps but then rises, ultimately forming the long-lived triplet. Figure 1B shows that the transient formed after 10 ps narrows on a sub-nanosecond time-scale to form the relaxed long-lived triplet. This spectral narrowing between singlet and triplet state TA is evident in the data at 690 nm (Figure 1C), where the rising triplet contribution is less marked than at 650 nm. These data provide the rationale for selecting 650 and 690 nm as resonant Raman pump wavelengths for FSRS (below), as they yield selectivity in probing singlet and triplet state Raman (Figure 1B-D).

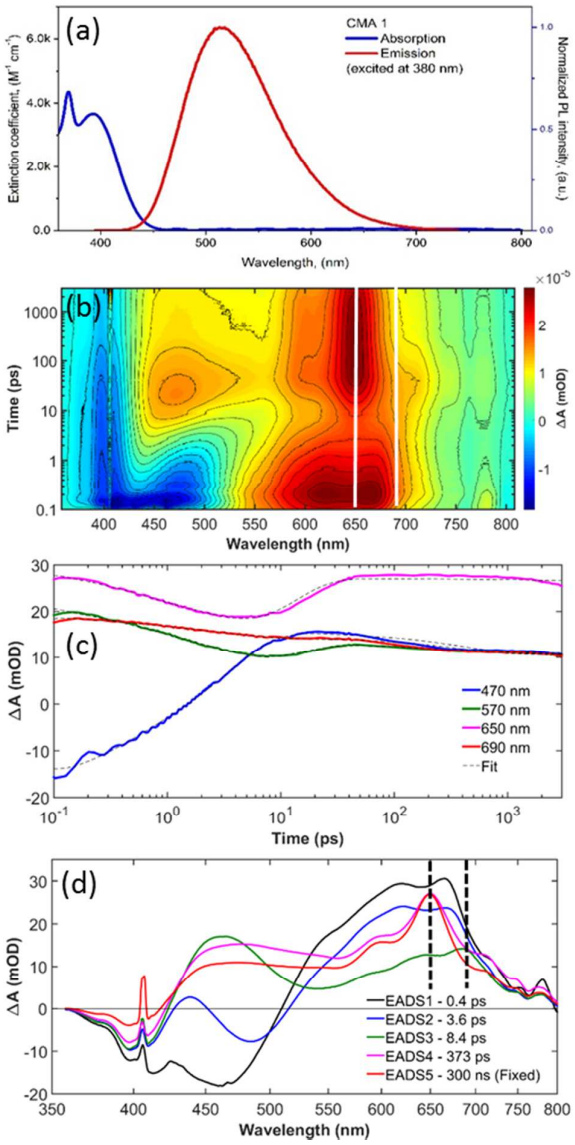

Figure 1 *Steady-state and transient electronic spectroscopy of CMA1 in chlorobenzene. (a) Steady-state absorption (blue) and emission (red). (b) Complete TA data set, plotted on a log timescale; the 650 and 690 nm wavelengths of the Raman pump are marked in white. (c) Transient kinetics at selected wavelengths 470 nm (blue) 570 nm (green) 650 nm (magenta) 690 nm (red); solid lines are data and dashed lines are the fit. The oscillation in the 470 nm data reflects coherently excited vibrational modes. (d) EADS recovered from the analysis of (b) in terms of a series of first-order steps: EADS1, (black) 0.4 ps; EADS2 (blue) 3.6 ps; EADS3 (green), 8.4 ps; EADS4 (magenta) 373 ps; Final EADS (red) 300 ns. Raman pump wavelengths used are again indicated by vertical dash lines.*

The TA data were subjected to global kinetic analysis in terms of successive first order rate constants.[14] The resulting evolution associated difference spectra (EADS) are shown in Figure 1D (fits to experimental data are included in Fig 1C). The expectation for a three level system exhibiting TADF (i.e. ground and excited singlet state, S_1, connected by an allowed transition, and a triplet state thermally coupled to S_1) is biexponential kinetics, with the fast component dominated by k_{ISC}^{-1} and slow reflecting the triplet lifetime, with amplitude depending on k_{RISC}. The data are more complex, requiring four first order steps leading to the final EADS.

The earliest EADS (EADS1) shows stimulated emission at 460 nm and broad TA between 500 and 750 nm, which relaxes with a 0.4 ps time constant to an intermediate, EADS2. EADS2 has the same TA as EADS1 but a red-shifted stimulated emission, revealing energy relaxation in S_1. We assign this to ultrafast structural evolution, consistent with the large Stokes loss (Figure 1A). EADS2 relaxes to EADS3 in 3.7 ps, a process dominated by conversion of the stimulated emission to TA between 450 and 500 nm, accompanied by decay of the broad S_1 absorption (650 nm); thus 3.7 ps reflects k_{ISC}^{-1}, in agreement with an earlier photoluminescence study.[4] EADS3 decays in 8.4 ps to EADS4, in which characteristic features of the triplet state begin to appear, notably around 650 nm. In addition the TA around 460 nm has flattened. There is further evolution from EADS4 in 373 ps, to populate the final spectrally narrowed feature at 650 nm, associated with the relaxed long-lived triplet; this does not evolve further on the nanosecond timescale. While the change from EADS4 is subtle it is apparent in the experimental data as continuing evolution up to 500 ps (Figure 1C).

The initial sub-picosecond spectral shift was assigned to fast structural reorganization in S_1; calculations on CMA2 (where Cu replaces Au) suggest a lengthening of the carbene C-N bond on excitation,[7] which could occur on this timescale. Solvation dynamics may also contribute, as calculations suggest a significant decrease in dipole moment on excitation.[6] However, the polar solvation spectral shift in weakly polar chlorobenzene is expected to be small, so the shift leading to EADS2 is more likely solute structural reorganization. Assignment of the 3.7 ps EADS2 to EADS3 relaxation to ISC is in excellent agreement with calculation.[8]

Later EADS (EADS3 to EADS5) reveal evolution between ISC and formation of the final relaxed triplet. The analysis recovers two relaxation phases, an initial fast one (8 ps) to an unrelaxed triplet, and a slower one (373 ps) forming the relaxed triplet state, which is coupled to emission through RISC. These relaxation processes are not accompanied by large spectral shifts, which might modify ΔE_{ST}, but reflect a structural relaxation, with resultant modulation of k_{RISC}. Calculations showed that excited state structural transformations, ligand twisting or deformation, occur on energetically flat or downhill surfaces, and that both singlet – triplet mixing and radiative transition moment are a function of these coordinates. We suggest that the intermediates observed here report on this structural evolution, and reflect changes in electronic structure accompanying state mixing. Such mixing may be promoted by rotation of the carbazolyl moiety;[6-7] diffusive orientational relaxation of molecules of similar size occur on the 10 – 100 ps timescale,[15] consistent with this mechanism.[6]

FSRS (Figure 2) provides access to Raman spectra of resonant excited states, and thus a route to structural dynamics. The tuneable narrowband (<10 cm^{-1}) 'Raman pump' pulse (see SI) was set at either 650 nm to be resonant with the narrow relaxed triplet state TA, or 690 nm to be resonant with S_1 (Figure 1B,D). We measure FSRS on the Stokes (Raman gain) side and the red side of the TA to yield simpler lineshapes.[16-17] Figure 2A displays time-resolved FSRS, reflecting formation of the relaxed triplet from the S_1 state, while Figure 2B plots the corresponding data for the broader underlying singlet state. That different resonance conditions favour one state over the other is evident in the time dependence; the amplitude of the spectra at 690 nm decay monotonically, while the 650 nm data increase with time. Thus early time data in Fig. 2B are characteristic of S_1, while later data in Fig. 2A reflect the triplet state Raman (earlier time 650 nm data has contributions from both). The degree of selectivity is demonstrated by evolution of the 436 cm^{-1} peak common to both states (Fig. 2C), with amplitude decaying at 490 nm but rising at 650 nm, reflecting the respective resonance condition (Figure 2B,D).

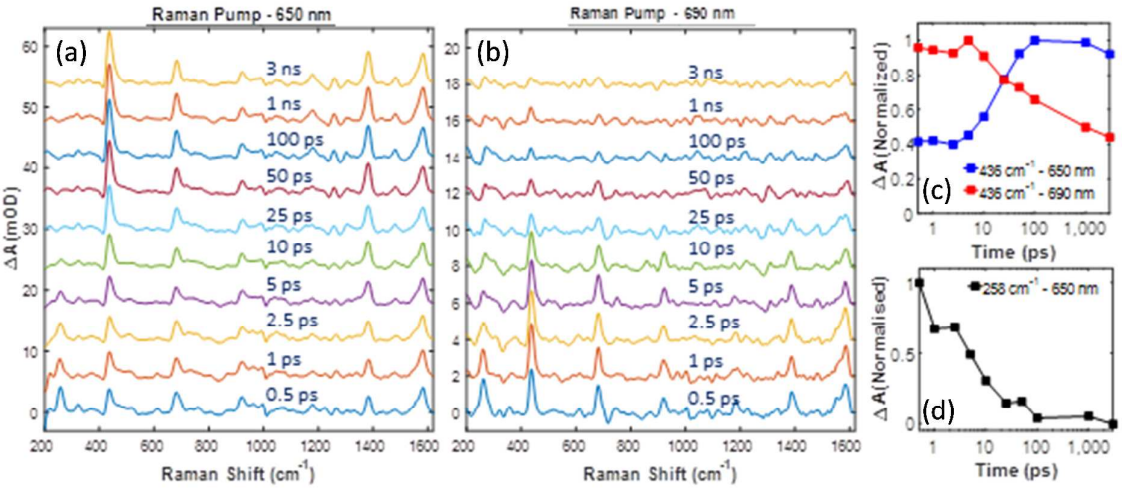

Figure 2 *FSRS data for CMA1 in chlorobenzene. (a) Stack plot of Raman spectra recovered with 650 nm Raman pump. (b) as for (a) but 690 nm Raman pump. (c) Time dependent signal of the 436 cm^{-1} amplitude for 690 nm (red) and 650 nm (blue) pump. (d) Time dependent FSRS signal at 258 cm^{-1} (650 nm pump).*

The ground state Raman of solid CMA1 has a cluster of intense modes at low wavenumber (<100 cm^{-1}) assigned to ligand torsion, and a further cluster above 1000 cm^{-1}, reflecting ring-stretch and CH bending modes.[4] The excited state spectra in Figure 2 are very different, with strong Raman activity at 258 and 436 cm^{-1} (where there is only weak ground state activity[4]) and additional modes in the ring-stretch region. These changes in vibrational spectra between ground and excited states point to a structure change. Calculations suggest that electronic excitation involves charge transfer from carbazole to carbene, accompanied by a decreased dipole moment.[4, 6] Such a change in electronic structure may give rise to modified bond strengths, manifested in vibrational spectra; in the absence of accurate calculations of excited state frequencies, more detailed assignment is not possible.

In contrast, Raman spectra of singlet and triplet states are very similar from 400 cm^{-1} to >1000 cm^{-1}; only the 1388 cm^{-1} peak undergoes a small (ca 5 cm^{-1}) red shift between singlet and triplet states, indicating weakening of a ring stretch in the carbazole ligand on ISC.[4, 6] This similarity implies similar

structures for the strongly mixed near degenerate S_1 and T_1 states. In general, the dominant contributions to the higher wavenumber Raman spectra probably arise from ligand ring localised modes, which are apparently not strongly perturbed on ISC.

The only striking difference between singlet and triplet states lies in their low-frequency Raman activity, where a strong 258 cm^{-1} mode makes a major contribution to the singlet state (690 nm), but decays in 8 ps (Figure 2D). This mode is also observed in the 650 nm data, but not beyond 10 ps, where the triplet is formed and stabilising. Thus, the 258 cm^{-1} mode reflects a distinct difference between singlet and triplet states. The 258 cm^{-1} matches calculations for carbazole ring modes which appear with low amplitude in the ground state spectrum. However, there is no reason to expect these modes to be absent in the triplet state or strongly resonantly enhanced. Its appearance specifically in S_1 could reflect intramolecular carbazole torsion relative to carbene,[6] following excitation of the nearly co-planar ground state (in which the 258 cm^{-1} mode is weak or absent[4]). However, that torsion potential is rather flat[6] and the ligand relatively massive leading to a calculated wavenumber in the ground electronic state of < 20 cm^{-1}, a much lower frequency than 258 cm^{-1}. A second source of low-frequency activity is modes involving the heavy Au ion. A recent calculation for CMA2 (M = Cu) pointed to excited state bending and elongation of the carbon-metal-nitrogen bond, enhancing spin-orbit coupling.[7] The structure changes associated with that relaxation could modulate low-frequency Raman activity. Thus, we tentatively assign the difference between S_1 and T_1 low-frequency Raman to structural changes reflected in C–Au–N localised modes upon change in electronic state.

In conclusion, we report ultrafast dynamics in the near ideal TADF molecule CMA1. Measurements of TA show a complex hierarchy including sub-picosecond structural relaxation and 3.7 ps ISC. This is followed by relaxation in the triplet state associated with the appearance of a new intermediate in <10 ps, and formation of the relaxed triplet state in hundreds of picoseconds, demonstrating structural dynamics in the triplet manifold. Structural evolution was interrogated by FSRS, which revealed marked difference between ground and excited states spectra, and between singlet and

triplet states, notably suppression of a strong low-frequency mode in S_1 on triplet state formation. It was suggested that this reflects structural relaxation around the central metal atom. These measurements are being extended to a range of CMAs.

Acknowledgment. S.R.M. is grateful to EPSRC for financial support (EP/N033647/1, EP/J009148/1, EP/R042357/1). M.B. is an ERC Advanced Investigator Award holder (grant no. 338944-GOCAT).

Supporting Information

Additional details on the TA and FSRS methodology, and an example of the background subtraction procedure required for the generation of the data in Figure 2.

References

1. Chen, T.; Zheng, L.; Yuan, J.; An, Z.; Chen, R.; Tao, Y.; Li, H.; Xie, X.; Huang, W. Understanding the Control of Singlet-Triplet Splitting for Organic Exciton Manipulating: A Combined Theoretical and Experimental Approach. *Sci. Rep.* **2015,** *5*, 10923.
2. Yang, Z. Y.; Mao, Z.; Xie, Z. L.; Zhang, Y.; Liu, S. W.; Zhao, J.; Xu, J. R.; Chi, Z. G.; Aldred, M. P. Recent advances in organic thermally activated delayed fluorescence materials. *Chem. Soc. Rev.* **2017,** *46*, 915-1016.
3. Chen, X. K.; Tsuchiya, Y.; Ishikawa, Y.; Zhong, C.; Adachi, C.; Brédas, J. L. A New Design Strategy for Efficient Thermally Activated Delayed Fluorescence Organic Emitters: From Twisted to Planar Structures. *Adv. Materials* **2017,** *29*, 1702767.
4. Di, D. W.; Romanov, A. S.; Yang, L.; Richter, J. M.; Rivett, J. P. H.; Jones, S.; Thomas, T. H.; Jalebi, M. A.; Friend, R. H.; Linnolahti, M.; et al. High-performance light-emitting diodes based on carbene-metal-amides. *Science* **2017,** *356*, 159-163.
5. Romanov, A. S.; Becker, C. R.; James, C. E.; Di, D. W.; Credgington, D.; Linnolahti, M.; Bochmann, M. Copper and Gold Cyclic (Alkyl)(amino)carbene Complexes with Sub-Microsecond Photoemissions: Structure and Substituent Effects on Redox and Luminescent Properties. *Chem. Eur. J.* **2017,** *23*, 4625-4637.
6. Foller, J.; Marian, C. M. Rotationally Assisted Spin-State Inversion in Carbene-Metal-Amides Is an Artifact. *J. Phys. Chem. Lett.* **2017,** *8*, 5643-5647.
7. Taffet, E. J.; Olivier, Y.; Lam, F.; Beljonne, D.; Scholes, G. D. Carbene-Metal-Amide Bond Deformation, Rather Than Ligand Rotation, Drives Delayed Fluorescence. *J. Phys. Chem. Lett.* **2018,** *9*, 1620-1626.
8. Thompson, S.; Eng, J.; Penfold, T. J. The intersystem crossing of a cyclic (alkyl)(amino) carbene gold (i) complex. *J. Chem. Phys.* **2018,** *149*, 014304.
9. Megerle, U.; Pugliesi, I.; Schriever, C.; Sailer, C. F.; Riedle, E. Sub-50 fs broadband absorption spectroscopy with tunable excitation: putting the analysis of ultrafast molecular dynamics on solid ground. *Appl. Phys. B* **2009,** *96*, 215-231.
10. Hall, C. R.; Conyard, J.; Heisler, I. A.; Jones, G.; Frost, J.; Browne, W. R.; Feringa, B. L.; Meech, S. R. Ultrafast Dynamics in Light-Driven Molecular Rotary Motors Probed by Femtosecond Stimulated Raman Spectroscopy. *J. Am. Chem. Soc.* **2017,** *139*, 7408-7414.
11. Kukura, P.; McCamant, D. W.; Mathies, R. A. Femtosecond stimulated Raman spectroscopy. *Annu. Rev. Phys. Chem.* **2007,** *58*, 461-488.
12. Hall, C. R.; Browne, W. R.; Feringa, B. L.; Meech, S. R. Mapping the Excited-State Potential Energy Surface of a Photomolecular Motor. *Angew. Chem. Int. Ed.* **2018,** *57*, 6203-6207.
13. Romanov, A. S.; Di, D. W.; Yang, L.; Fernandez-Cestau, J.; Becker, C. R.; James, C. E.; Zhu, B. N.; Linnolahti, M.; Credgington, D.; Bochmann, M. Highly photoluminescent copper carbene complexes based on prompt rather than delayed fluorescence. *Chem. Commun.* **2016,** *52*, 6379-6382.
14. Snellenburg, J. J.; Laptenok, S. P.; Seger, R.; Mullen, K. M.; van Stokkum, I. H. M. Glotaran: A Java-Based Graphical User Interface for the R Package TIMP. *J. Stat. Software* **2012,** *49*, 1-22.
15. Hartman, R. S.; Konitsky, W. M.; Waldeck, D. H.; Chang, Y. J.; Castner, Jr., E. W. Probing solute–solvent electrostatic interactions: Rotational diffusion studies of 9,10-disubstituted anthracenes. *J. Chem. Phys.* **1997,** *106*, 7920-7930.
16. Umapathy, S.; Mallick, B.; Lakshmanna, A. Mode-dependent dispersion in Raman line shapes: Observation and implications from ultrafast Raman loss spectroscopy. *J. Chem. Phys.* **2010,** *133*, 024505.
17. Oscar, B. G.; Chen, C.; Liu, W. M.; Zhu, L. D.; Fang, C. Dynamic Raman Line Shapes on an Evolving Excited-State Landscape: Insights from Tunable Femtosecond Stimulated Raman Spectroscopy. *J. Phys. Chem. A* **2017,** *121*, 5428-5441.